

# Carbonates in Zeolites: Formation, Properties, Reactivity

Andrey A. Rybakov,<sup>\*[a]</sup> Ilya A. Bryukhanov,<sup>[b]</sup> Alexander V. Larin,<sup>[a]</sup>  
and Georgy M. Zhidomirov<sup>[a,c]</sup>

Two possible schemes of carbonate formation (with and without water participation) in cationic form zeolites are considered. Activation energy for the formation of hydrogen carbonate in NaX zeolite from water and carbon dioxide is calculated at the DFT level with periodic boundary conditions, while the problems of modeling the formation of symmetric carbonate in the same zeolite are discussed. The formation of copper carbonate is studied using binuclear CuOCu clusters

from CO<sub>2</sub> where the influence of water on the barrier is discussed. The questions related to DFT application to binuclear copper clusters are also considered by comparison with the data obtained at the MP2 level. The reactivity of copper carbonate is tested in the reaction with methanol. © 2015 Wiley Periodicals, Inc.

DOI: 10.1002/qua.24994

## Introduction

The perspective of using CO<sub>2</sub> instead of hydrocarbons as the source of carbon accelerated the studies of the processes related to CO<sub>2</sub> behavior in perspective systems for separation and/or which can serve as a reaction media. Considering the large required tonnages of future industries, one can assume that necessity of recycling coproducts and catalysts increases the attractiveness of using natural materials with comparable performance, such as zeolites instead of metal-organic frameworks. Recent finding of template-free way for the synthesis of faujasite-type (FAU) zeolites of variable Si/Al modulus<sup>[1]</sup> have to increase their availability for the wider area of possible applications. Their use for separation of CO<sub>2</sub> mixtures remains an attractive perspective owing to rather large available volume of the FAU pores. However, carbonate formation on a moderate Si/Al modulus can be a reason of partial blockage of FAU pores for gas adsorption.<sup>[2,3]</sup> The authors<sup>[2]</sup> noted that excluded volume for CO<sub>2</sub> adsorption in CsY corresponds to five molecules per unit cell at CO<sub>2</sub> pressure of 14 bar and temperature of 303 K. Respective detailed experimental evaluations were analyzed by Calero's group for H<sub>2</sub> adsorption in NaX (FAU zeolite), NaA, NaCaA (LTA zeolite).<sup>[3]</sup> However, all the results of this work related to modeling of adsorption have been performed without addressing to microscopic picture of carbonates discussed using density functional theory (DFT)<sup>[4–7]</sup> or molecular mechanic<sup>[8]</sup> approaches. Microscopic models of carbonate species were optimized and discussed for the NaKA,<sup>[4,5]</sup> NaX,<sup>[7,8]</sup> MeRHO,<sup>[6]</sup> MeMOR<sup>[5]</sup> zeolites, Me = Li, Na, K, Cs, Mg, Ca, Ba, and a wide set of cluster models with diversified geometries (8R, 6R+4R, 10T) and similar cations.<sup>[5]</sup> More precisely, one has considered the thermodynamic aspect of formation of carbonates and hydrogen carbonates in MeRHO forms regarding various alkaly forms and Si/Al ratio.<sup>[6]</sup> The heats of their formation were found to be exothermic ones for hydrogen carbonates at any Si/Al ratio. For carbonates, the sign of the heat depends on the alkaly cation type (Li, Na, . . .) and the Si/Al ratio. The activation energies for car-

bonate formations were not studied yet for any carbonate or hydrogen carbonate form. NaX or 13X is a promising system owing to its available volume throughout the FAU types.<sup>[3]</sup> In this work, we will calculate the activation energies for NaX, where an easy formation of asymmetric carbonates, which may be hydrogen carbonates, is well-confirmed experimentally as well as their transformation to the symmetric form.<sup>[9–11]</sup>

In parallel, the authors<sup>[12,13]</sup> have confirmed the possible catalytic activity of formates whose presence in CuY was defined as one of the factors that prompts dimethylcarbonate (DMC) formation. The DMC is an important addition for motor fuels as well as methylating agent for industry so that respective methods of its production are under detailed studies.<sup>[12,13]</sup> The formates possess experimental bands 1580 and 1354 cm<sup>-1</sup> with the difference between the higher and lower valence vibrations of HCOO<sup>-</sup> or band splitting (BS) of 226 cm<sup>-1</sup><sup>[12]</sup> or 1590 and 1369 cm<sup>-1</sup> (BS = 221 cm<sup>-1</sup>) in the later work<sup>[13]</sup> where wide asymmetric peaks with 1620 and 1350 cm<sup>-1</sup> (the difference between the higher and lower valence CO<sub>3</sub><sup>-2</sup> vibrations or BS = 270 cm<sup>-1</sup>) were assigned to carbonates (Fig. 10 in Ref. [12]). However, bidentate carbonates with different BS values can be optimized as a series of multication clusters<sup>[6]</sup> that is why one can suspect that these formates could be just carbonates with another geometry than those observed with the BS of 270 cm<sup>-1</sup>.<sup>[4–8]</sup> As a result, the copper carbonates require to be tested as reagents for the DMC syntheses.

[a] A. A. Rybakov, A. V. Larin, G. M. Zhidomirov  
Department of Chemistry, Moscow State University, Leninskie Gory, GSP-2,  
Moscow 119992, Russia  
E-mail: rybakovy@gmail.com

[b] I. A. Bryukhanov  
Department of Mechanics and Mathematics, Moscow State University,  
Leninskie Gory, GSP-2, Moscow 119992, Russia

[c] G. M. Zhidomirov  
Quantum Chemistry Department, Boreskov Institute of Catalysis SB RAS,  
Novosibirsk, 630090, Russia

Contract grant sponsor: RFFI; contract grant number: 12-03-00749a, 14-01-00310a.

© 2015 Wiley Periodicals, Inc.

Respective BS values throughout all carbonates were analyzed as a function of their geometries expressed via asymmetry parameter  $\delta$  or bond distortion:

$$\delta = \sum_{i=1-3} (||C-O|_i - |C-O|_{\text{aver}}|) \quad (1)$$

relative to the average value  $|C-O|_{\text{aver}} = (\sum_{i=1-3} |C-O|_i)/3$  in the carbonate.<sup>[5]</sup> It was found that  $\delta$  correlates with the BS or the difference between symmetric and asymmetric vibrational frequencies of the carbonate anion with a minor dependence on a computational level and the cation type.<sup>[5]</sup> The “ $\delta$ -BS” dependences for carbonates and hydrogen carbonates are, however, different<sup>[6]</sup> but the first one can qualitatively describe the BS( $\delta$ ) for monomethylcarbonates and dimethylcarbonates. We shall use this parameter in the discussion below.

In the following parts, we shall consider calculation of activation energies of the carbonate formation from CO<sub>2</sub> and H<sub>2</sub>O in NaX regarding periodic boundary conditions (PBC) (The activation energy and accompanying factors of HCO<sub>3</sub><sup>-</sup>/CO<sub>3</sub><sup>-2</sup> formation section). Then, some aspects of DFT application to the binuclear copper CuO<sub>x</sub>Cu clusters, X = 1–2, will be presented as well as to modeling of carbonates (Problem of multiplicity of the ground electronic state of CuO<sub>x</sub>Cu section). The Cu-carbonate formation reaction section is devoted to the second possible route of the formation of Cu-carbonates from CuO<sub>x</sub>Cu with and without water. The carbonate reactivity will be tested in the reaction with methanol (Modeling reaction between Cu-carbonates and CH<sub>3</sub>OH section) which is of interest as a first step for DMC formation.

## Computational Details

Zeolite fragments were modeled with Gaussian 09<sup>[14]</sup> using isolated clusters consisting of 8R and extended (8RL) rings cut from MOR zeolite, cluster with two 6R and 4R windows (6R+4R) cut from FAU, and the 10T cluster from Ref. [15]. All ruptured T–O bonds of all T atoms (T = Al, Si) were capped by hydrogen atoms, the procedure is described in more detail in Refs. [5,16–19]. Reagents and products have been optimized at the isolated cluster level considering DFT hybrid B3LYP, wB97XD with improved presentation of the dispersive terms<sup>[20]</sup> with the LANL2DZ(Cu)/6-31G\*(H, Al, Si, C, O, H) basis sets. Testing the pseudopotential LANL2DZ(Cu) basis set was done by a comparison with TZVP(Cu) for some examples (both for geometry and activation energy).<sup>[14]</sup>

The CuMOR structure (the chemical composition of the unit cell is Cu<sub>2</sub>Al<sub>2</sub>Si<sub>46</sub>O<sub>97</sub>) has been considered because it allows formation of the centers, probably, of the CuOCu type, which oxidize CH<sub>4</sub><sup>[15,21–23]</sup> and is involved in the carbonylation with a moderate yield,<sup>[24]</sup> while the carbonylation is the target for the next step calculations. The carbonate formation from CO<sub>2</sub> and H<sub>2</sub>O has been considered in NaX model (the chemical composition of the unit cell is Na<sub>24</sub>Al<sub>24</sub>Si<sub>24</sub>O<sub>96</sub>). Plane wave computations with the PBC using the PBE,<sup>[25]</sup> PBEsol,<sup>[26]</sup> and PW91<sup>[27]</sup> functionals within the projector augmented wave (PAW) method<sup>[28]</sup> were performed with VASP.<sup>[29,30]</sup> QST3<sup>[14]</sup> at the isolated cluster level and nudged elastic bands (NEB)<sup>[31]</sup> method

at the PBC level have been, respectively, used for a search of the transition state (TS). The scripts provided by the Transition State Tools for VASP were used to build the images for the NEB calculations.<sup>[31]</sup> The energy cutoff was set to 500 eV. The Brillouin zone *k*-sampling was restricted to the  $\Gamma$ -point for the geometry optimization and frequency calculation. Figures of zeolites were realized with MOLDRAW2.0.<sup>[32]</sup>

## Results

Two possibilities of carbonate formation were considered in our work. The first case relates to the reaction between water and carbon dioxide (Fig. 1a), while the second one is the trapping of carbon dioxide by CuOCu species (Fig. 1b). The interactions of the second type pass via a barrierless route for earth alkaline (EA) cationic MeO<sub>x</sub>Me clusters,<sup>[16]</sup> Me = Mg, Ca, Sr, Ba, X = 1–2\*, but not for copper CuOCu moieties. Earlier, we have studied the carbonate formation due to the CO oxidation over EA oxide MeO<sub>x</sub>Me clusters,<sup>[17,18]</sup> where a barrier cannot be determined due to an immediate CO<sub>3</sub><sup>-2</sup> anion incorporation between two Me cations.

### The activation energy and accompanying factors of HCO<sub>3</sub><sup>-</sup>/CO<sub>3</sub><sup>-2</sup> formation

The reaction of HCO<sub>3</sub><sup>-</sup> formation was modeled in NaX where its presence was confirmed.<sup>[9–11]</sup> The NaII position in a 6R window (Fig. 1c) was selected as adsorption site for both CO<sub>2</sub> and H<sub>2</sub>O. Along the reaction coordinate one observes the decrease of the distance between C atom of CO<sub>2</sub> and O atom of H<sub>2</sub>O in parallel with the transfer of water proton toward O atom of the 6R ring. It is also accompanied by slow angular deformation of CO<sub>2</sub> axis and a deviation of Na cation from the 6R plane of three nearest O atoms. The modeling with PBC leads to a moderate barrier of 16.8 kcal/mol (Fig. 2) and 12.9 kcal/mol at the PBE and PBEsol levels that do not justify the fast reaction at room temperature but it gives a correct order of value for the process. The PW91 functional provides the values being similar to that obtained using PBE (Table 1). In all the cases, the coordinate of the reaction corresponds to vibrations of the O atom of water molecule (animation “03-TS.avi” file related to the PBE level is given in Supporting Information). It is characterized by a close location of three Na cations around and is accompanied by the large drift of one NaIII(121) cation whose displacement is shown in Table 2. Regarding the minor shift of the NaII<sup>+</sup> cation in its closest 6R, the cationic displacements are convenient to be calculated relative to this NaII<sup>+</sup> cation. One of the cations approaches NaII at the reaction center by 1.404 Å while the second was displaced slightly far from NaII by –0.085 Å (column in Table 2). The new location of the cations nearly at middle points between the O<sub>c</sub> atoms of carbonate and O<sub>z</sub> ones of the framework equilibrates the Na<sup>+</sup> interactions with them, thus performing shielding function for Coulomb O<sub>c</sub>–O<sub>z</sub> repulsion. More precisely, the distances between the Na121 (given in column 4 of Table 2— $\Delta R = 3.620$  Å) and O<sub>c</sub> atoms (2.377,

\*Reaction with CaO<sub>2</sub>Ca have been also studied which produces singlet dioxygen as coproduct.<sup>[16,17]</sup>

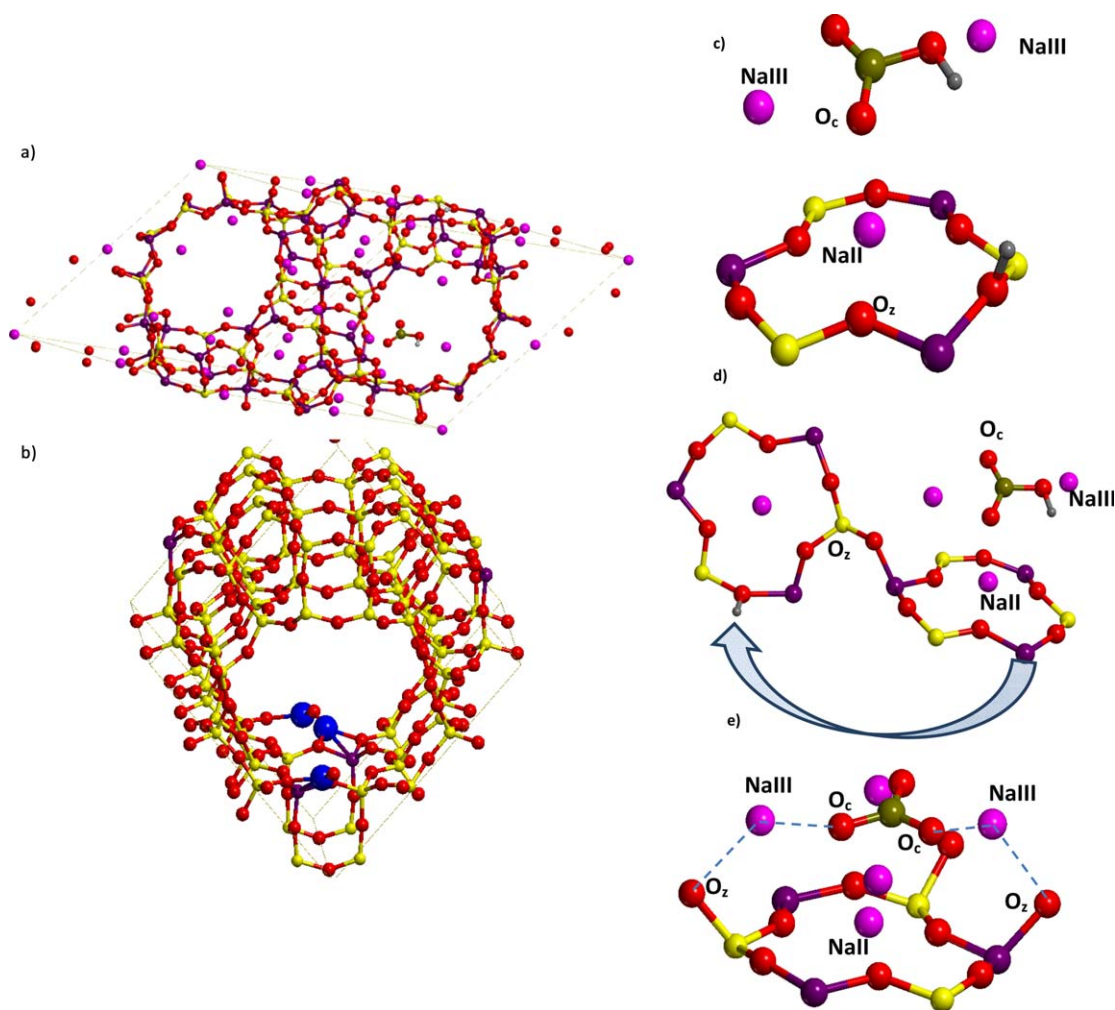


**Figure 1.** Geometries of NaX a) and (CuOCu)MOR b) zeolite frameworks including local geometries of (c, d)  $\text{HCO}_3^-$ , (e)  $\text{CO}_3^{2-}$  carbonates formed at the NaII site in NaX or of the carbonate after (c) reaction or obtained by (d, e) embedding and optimization using VASP5.3.3 at the PBE/PAW level. The  $\text{O}_z$  notations for oxygen atoms of the NaX framework or  $\text{O}_c$  for the carbonate O atoms are shown. The arrow shows the proton shift obtained after reaction (d), see the text for explanation. The atomic colors are given in magenta light, blue, red, yellow, magenta, and gray for Na, Cu, O, Si, Al, and H, respectively.

2.817 Å) are close to those between Na121 and  $\text{O}_z$  (2.353, 2.585 Å) of the nearest 4R. Analogically, Na116 cation (given in column 4 of Table 2— $\Delta R = 5.390$  Å) has two neighbors of the  $\text{O}_c$  (2.379 Å) and  $\text{O}_z$  (2.369 Å) types, the second one belongs to the nearest 4R ring (Table 3).

The endothermic and exothermic heats of 1.9 kcal/mol (Fig. 2) and  $-2.8$  kcal/mol (Table 1) are thus obtained in NaX (Si/Al = 1) at the PBE and PBEsol levels, respectively, being minor values (in absolute value) relative to the exothermic heat of  $-22.5$  kcal/mol earlier calculated for  $\text{HCO}_3^-$  formation in the Na6RHO zeolite (Si/Al = 3).<sup>[6]</sup> The heat dependence of  $\text{HCO}_3^-$  formation versus Si/Al (Fig. 4 in Ref. [6]) predicts a smaller heat (in absolute value) with Si/Al. The reason for the opposite trend comes from the different models used to evaluate the heats of  $\text{HCO}_3^-$  formation in both NaX (herein) and Na6RHO (in Ref. [6]) cases. In Ref. [6], a full reaction between  $\text{CO}_2$  and  $\text{H}_2\text{O}$  has not been realized, but a final optimized model of the product in Na6RHO, that is, proton and  $\text{HCO}_3^-$  separated by a large distance between them, has been proposed. We have repeated this approach (column 5 in Table 2) herein by a similar modifi-

cation of the model moving the proton by as much as 11.2 Å to the remote 6R position (NaII) in the neighbor cage of NaX (shown by arrow in Fig. 1d). Full relaxation of the system led to the heat  $\Delta U$  of  $-23.6$  kcal/mol which is close to the heat of  $-22.5$  kcal/mol calculated in NaRHO (Si/Al = 3). Both nearest NaIII cations vary very slightly in their positions in the course of the following optimization remaining at the middle sites between the closest  $\text{O}_c$  and  $\text{O}_z$  atoms (Table 3), that is, Na116... $\text{O}_c$  (2.341 Å) and Na116... $\text{O}_z$  (2.348 Å) and Na121... $\text{O}_c$  (2.433, 2.437 Å) and Na121... $\text{O}_z$  (2.313, 2.707 Å) (Table 3).

As  $\text{CO}_3^{2-}$  formation was also observed experimentally in  $\text{NaX}^{[9-11]}$  we have tried to obtain from  $\text{HCO}_3^-$  due to loss of proton but have not finally succeeded. Respective reasons of our failure become evident if one repeats an optimization of  $\text{CO}_3^{2-}$  in the same way (without a reaction from  $\text{CO}_2$  and  $\text{H}_2\text{O}$ ) distributing two protons over the framework (Table 2, Fig. 1e) has done herein for  $\text{HCO}_3^-$ . As a result, four NaIII<sup>+</sup> cations diffuse (in a barrierless way) toward the  $\text{CO}_3^{2-}$  moiety while only two NaIII<sup>+</sup> cations move to  $\text{HCO}_3^-$  (and with a smaller amplitude, see Table 2). Each  $\text{Na}^+$  cation finds a new intermediate

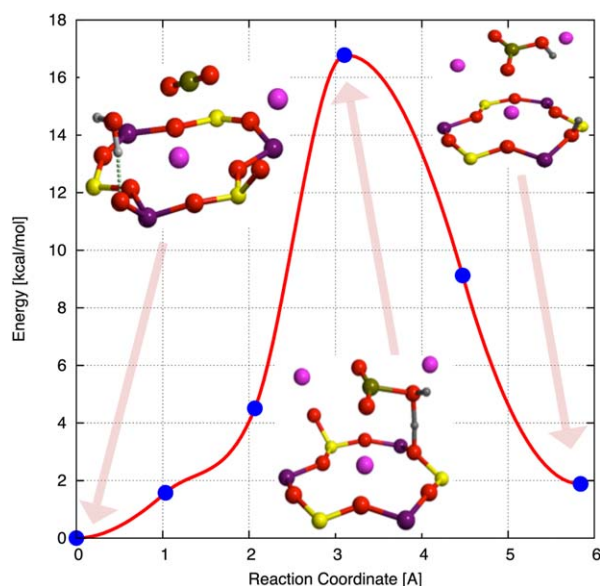


**Figure 2.** Energy (kcal/mol) versus reaction coordinate (Å) including as insets the geometries of reagent, TS, and product of the reaction between  $\text{CO}_2$  and  $\text{H}_2\text{O}$  at the NaII site of the NaX framework optimized using VASP5.3.3 at the PBE/PAW level. The atomic color agreement is given in Figure 1.

position between  $\text{O}_c$  and  $\text{O}_z$  atoms in the same manner as for  $\text{HCO}_3^-$  (Table 3). These changes after the cationic diffusion are also illustrated regarding the Bader charges (Table 4). Two important issues can be extracted from these charge calculations being useful for following Monte Carlo (MC) or molecular dynamics (MD) modeling: (1) the variations of the charges in the presence of the carbonates and (2) the charge of  $\text{O}_c$  carbonate atoms relative to the  $\text{O}_z$  ones in the NaX frameworks. According to the proposed modified force field (FF),<sup>[3]</sup> the  $\text{O}_z$  and Na charges become larger in absolute values, that is, from  $-0.41384 e^{[33]}$  to  $-0.4838 e$  in NaA and  $-0.4372 e$  in NaCaA for  $\text{O}_z$  charge at the Si– $\text{O}_z$ –Al case and from  $0.3834 e^{[33]}$  to  $0.6633 e$  in NaA and  $0.4767 e$  in NaCaA for Na charge.<sup>[3]</sup> Analyzing Table 4, one can note a slight variation (decrease is more frequent than increase) of the  $\text{O}_z$  charges depending on the carbonate presence and the location of the cations. Maximum changes are  $-0.021 e$  for Na and  $0.019 e$  for  $\text{O}_z$  atom in the nearest 6R. The charges of  $\text{O}_z$  atoms are larger than those of  $\text{O}_c$  atoms in 1.3 times. The slight variation of Bader atomic charges on addition of carbonates is a convenient feature facilitating an application of MC or MD approaches to the carbonates in zeolites.<sup>[8]</sup> These estimates are important for adsorption modeling

**Table 1.** The heat of  $\text{HCO}_3^-$  formation reaction ( $\Delta U$ ), activation energy ( $E_a$ ), and the imaginary frequency ( $-i\omega$ ) of the TS in NaX for different DFT functionals.

Units Functional	$\Delta U$		$E_a$		$-i\omega$ $\text{cm}^{-1}$
	eV	kcal/mol	eV	kcal/mol	
PBE	0.082	1.8	0.728	16.8	401.7
PBEsol	-0.121	-2.8	0.560	12.9	317.3
PW91	0.081	1.9	0.725	16.7	399.9

when authors try to consider a new set of the charges to take into account the presence of carbonates. The first work of such type was, however, successfully performed varying the atomic charges of respective FF without exact microscopic model of carbonates.<sup>[3]</sup>

The example of carbonates in NaX provides us an occasion to test the extrapolation of linear dependence  $\Delta U(R) = (-0.861 + 0.223 \times R) \times 23.06$  for  $\text{CO}_3^{2-}$ , where  $R = \text{Si}/\text{Al}$  (Fig. 4 in Ref. [6]), to the point  $R = 1$  (NaX). One reminds that linear approximation of the heat versus Si/Al was fitted within  $2.43 < R < 7$  for a series of NaCsRHO models. This function results in  $\Delta U = -14.7$  kcal/mol for NaX that is in a reasonable agreement with  $-15.4$  kcal/mol calculated using VASP. Analogous prediction of the extrapolated  $\Delta U$  value of  $-33.1$  kcal/mol via linear dependence  $(-1.533 + 0.098 \times R) \times 23.06$  (Fig. 4 in Ref. [6]) for  $\text{HCO}_3^-$  in NaX ( $R = 1$ ) is less accurate, as one has calculated value of  $-23.6$  kcal/mol. Nevertheless, we can confirm that the extrapolation of the linear dependences of  $\Delta U(R)$  leads to a correct order of values in a wide  $R$ -range for both  $\text{HCO}_3^-$  and  $\text{CO}_3^{2-}$ . An unexplained aspect of the  $\Delta U$  extrapolation is the absence of such (Na, Cs)-carbonates in the RHO frameworks where only Li-carbonates were registered by infrared spectroscopy (IR).<sup>[34]</sup> In this sense, we believe that heavier carbonates in RHO can be discovered in the future because the same DFT/PBE/PAW approach is capable to properly explain (in agreement with an absence of IR peaks in the experiment<sup>[2]</sup>) the thermodynamically forbidden (i.e., the variation of reaction energy  $\Delta E > 0$ ) Li- and Na-carbonates in the FAU framework of similar Si/Al modulus (2.5).<sup>[35]</sup>

The stabilization of  $\text{CO}_3^{2-}$  deserves a short comment. The intuitive explanation of easier formation of  $\text{HCO}_3^-$  with higher exothermic effect compared with  $\text{CO}_3^{2-}$ <sup>[8]</sup> is the smaller charge of  $\text{HCO}_3^-$  ( $-0.868$  against  $-1.690 e$  in Table 4). The higher charge should be related to the large quantity (four) of NaIII cations shifted by an essential vector of  $1.404 \text{ \AA}$  and more (Table 2) to optimize chemisorbed  $\text{CO}_3^{2-}$ . It leads to a deeper reordering of remote cations than those required for  $\text{HCO}_3^-$  (a large displacement of only one cation, see columns 4 or 5 in Table 2). This is in agreement with the high amplitudes of cationic displacements relative to their crystallographic sites calculated earlier in MeRHO zeolites<sup>[6]</sup> where relative Na...Na distances for Me = Na case are shown with (Fig. 1e) and without (Supporting Information Fig. S1i)  $\text{CO}_3^{2-}$ . Such concert movements of many particles, forming a reaction coordinate, can explain why we failed to transform  $\text{HCO}_3^-$  to  $\text{CO}_3^{2-}$  that requires parallel motions of many species. Such complex reaction can be hardly reproduced due to a limited set of the images even with NEB algorithm which could drive the system via a predefined series of intermediate geometries. Only a close coupling of such modes for many particles could occasionally result in the successful construction of the TS.

#### Problem of multiplicity of the ground electronic state of $\text{CuO}_x\text{Cu}$

As we mentioned in introduction, the copper carbonates require to be tested as reagents and/or catalyst for the DMC

**Table 2.** The energies (in kcal/mol),  $(\text{CO}_3^{2-})\text{Na}ll \dots \text{Na}ll$  distances ( $R$ , in Å), where  $\text{Na}ll$  is sodium atom in 6R ring being the closest to the carbonate, with and without carbonates ( $\text{HCO}_3^-$ ,  $\text{CO}_3^{2-}$ ) and its decrease ( $\Delta R$ , in Å) in the  $\text{Na}X$  zeolite after reaction (column 4) or obtained by embedding and optimization (columns 3, 5) as calculated using VASP5.3.3 at the PBE/PAW level.

NaIll	No carbonates	+ $\text{CO}_3^{2-}$ (embedding)		+ $\text{HCO}_3^-$ (reaction)		+ $\text{HCO}_3^-$ (embedding)	
	$R$	$R$	$\Delta R$	$R$	$\Delta R$	$R$	$\Delta R$
1	2	3		4		5	
116	5.305	3.873	1.432	5.390	-0.085	5.239	0.066
121	5.001	3.178	1.823	3.692	1.404	3.620	1.381
124	6.393	3.620	2.773	-	-	-	-
125	5.070	3.666	1.404	-	-	-	-
Energy			-15.4		2.3		-23.6

The numbers of the columns are used in the text.

syntheses. First, we would like to comment the difference between the results of the computations of  $\text{CuO}_x\text{Cu}$  species at the hybrid (B3LYP) or generalized gradient approximation (GGA) (PW91) DFT and MP2 levels and why the DFT approach used herein is applicable. The ESR signal of  $\text{Cu}^{2+}$  in Cu-form zeolites is not usually supported by additional components<sup>[36,37]</sup> which could be assigned to the total spin moment of the  $[\text{CuOCu}]^{2+}$  fragment. Even if such signal was once assigned to  $[\text{CuOCu}]^{2+}$  in  $\text{CuY}^{[37]}$  the later works performed on  $\text{CuZSM-5}^{[38]}$  did not confirm this possibility. Most probably it indicates the singlet state of the  $\text{CuOCu}$  species. As was shown experimentally using high resolution X-ray for  $\text{CuO}_2\text{Cu}^{[39]}$  it possesses singlet ground state in the 6-type model (according to the classification in Ref. [40] or the 2-type model in Ref. [41]), that is, plain rhombohedra with O—O bond, with  $|\text{Cu} \dots \text{Cu}| = 3.54$  Å and  $|\text{O-O}| = 1.41$  Å in the complex with four-coordinated Cu atoms with two external N-oriented ligands ( $|\text{Cu-N}|$  is between 1.95 and 2.10 Å). Third, N-ligands for each  $\text{Cu}^{2+}$  are remote as much as 2.66–2.77 Å above/below the plane of the  $[\text{CuO}_2\text{Cu}]^{2+}$  fragment. The extremely important role of super-exchange between cations and ligands is confirmed by the result that the agreement between the DFT computations and the experimental data<sup>[39]</sup> is only achieved if the Cu coordination is enough complete.<sup>[42]</sup>

The cluster calculations at the MP2 level demonstrate that the energy of singlet state is lower, while all the applied DFT functionals show that the energy of triplet state is lower for any cluster or periodic solution (Table 5). Additionally, we have extended the 8R model up to the larger 8RL cluster that corresponds to 16 additional O atoms connected to eight T = Al,

Si atoms in 8R ring. For this model, the smaller difference of 13.8 kcal/mol between singlet and triplet states instead of 19.4 kcal/mol for 8R was obtained, but the energy of the singlet state remains lower at the MP2 level (Table 5). This different singlet–triplet ratio between MP2 and DFT remains for all the studied examples of the  $\text{CuO}_2\text{Cu}$  species as well including the largest 10T cluster from the Ref. [15] (Table 5).

All the  $\text{CuOCu}$  species have been optimized leading to the final Cu—O—Cu angles from 135.09 to 147.19° at the distances between 3.295 and 3.947 Å (Table 6). The latter are longer than the range studied by Goodman et al. using the cluster cut from ZSM-5 structure (from 2.69 to 2.81 Å from Table 1 of the Ref. [40]). The LSDA solution with GGA corrections (BP86) was applied with the Slater type basis set of the DZ quality<sup>[40]</sup> using the ADF code. The Figure 5 from Ref. [40] predicts that the energy of the singlet state  $^1A$  is lower if the Cu—O—Cu angle is smaller than  $\sim 157^\circ$ . The shorter Cu...Cu interval in Ref. [40] compared with that in our work (Table 7) could be the reason that we obtained lower energy of the triplet states with any DFT functional. This singlet–triplet inversion is repeated in simulations with VASP 5.3.3 using PBC and various DFT functionals (Table 5). The ground triplet state is conserved but the difference drops further up to -1.4, -1.0, and -0.4 kcal/mol at the PW91,<sup>[27]</sup> PBEsol,<sup>[26]</sup> and PBE<sup>[25]</sup> levels, respectively, using PAW approach<sup>[28]</sup> in all the cases with VASP.<sup>[29,30]</sup> The extension of the cluster and the solution with PBC thus decreases the singlet–triplet energy difference but not changes its sign.

The angular ( $\text{CuO}_2\text{Cu}$ ) dependence of the multiplet states<sup>[40,41]</sup> was studied within wider Cu...Cu interval in Ref. [33] at the DFT level going outside the interval, which is characteristic one for the

**Table 3.** The  $\text{Na}ll \dots \text{O}$  distances (in Å), where  $\text{O}_c$  and  $\text{O}_z$  oxygen atoms are related to carbonate or framework, respectively, with and without carbonates ( $\text{CO}_3^{2-}$ ) in the  $\text{Na}X$  zeolite after reaction (column 3) or obtained by embedding and optimization (columns 2, 4) as calculated using VASP5.3.3 at the PBE/PAW level.

NaIll	+ $\text{CO}_3^{2-}$ (embedding)		+ $\text{HCO}_3^-$ (reaction)		+ $\text{HCO}_3^-$ (embedding)	
	$\text{O}_c$	$\text{O}_z$	$\text{O}_c$	$\text{O}_z$	$\text{O}_c$	$\text{O}_z$
1	2		3		4	
116	2.191	2.305	2.341	2.348	2.379	2.369
121	2.296, 2.570	2.469	2.433, 2.437	2.313, 2.707	2.377, 2.817	2.353, 2.585
124	2.226	2.452, 2.474	-	-	-	-
125	2.279, 2.397	2.318	-	-	-	-

The numbers of the columns are used in the text.

**Table 4.** Bader type charges ( $Q$ , e) of the framework atoms and their variations ( $\Delta Q$ , e) including the Na cations located closely to the carbonate (110, 116, 121, 124, 125), far from it (108, 109, 111), O<sub>2</sub> atoms of the nearest 6R window (108, 109, 111) and of an remote 6R window (30, 33, 34) of one or two protons (1, 2) and of the O<sub>c</sub> atoms (100, 101, 102) of hydrogen carbonate and carbonate, respectively, calculated at the PBE/PAW level.

Atom	$Q(+CO_3^{2-})$	$\Delta Q$	$Q$	$\Delta Q$	$Q(+HCO_3^-)$
Na 110	0.829	-0.010	0.839	-0.004	0.835
Na 116	0.856	-0.015	0.881	-0.014	0.867
Na 121	0.860	-0.010	0.870	0.005	0.875
Na 124	0.856	-0.011	0.867	0.000	0.867 <sup>[a]</sup>
Na 125	0.856	-0.021	0.877	0.000	0.877 <sup>[a]</sup>
Na108	0.834	-0.006	0.840	0.000	0.840
Na109	0.836	0.002	0.834	0.004	0.838
Na111	0.838	-0.001	0.839	0.002	0.841
O30	-1.609	0.002	-1.611	0.002	-1.609
O33	-1.619	0.001	-1.620	0.019	-1.601
O34	-1.608	0.006	-1.614	-0.001	-1.615
C3	2.091	-	-	-	2.099
O100	-1.251	-	-	-	-1.209
O101	-1.262	-	-	-	-1.235
O102	-1.268	-	-	-	-1.121 <sup>[b]</sup>
H1	0.664	-	-	-	0.598 <sup>[c]</sup>
H2	0.644	-	-	-	0.622
CO <sub>3</sub> /HCO <sub>3</sub>	-1.690	-	-	-	-0.868

[a] Proton holds its position. [b] O atom of hydroxyl group in HCO<sub>3</sub><sup>-</sup>. [c] Proton of hydroxyl group in HCO<sub>3</sub><sup>-</sup>.

cluster cut from ZSM-5 structure, being limited by the shorter Cu...Cu distances from 2.45 to 2.83 Å (Table 1 of the Ref. [40]). Despite of the studied variety of the CuO<sub>2</sub>Cu geometries in Ref. [40], we have obtained similar ground singlet state models for the 8R and 6R+4R clusters at the MP2 level (Table 6). They should be classified as the puckered (nonplain rhombohedra) or the 8 type according to the classification induced by Goodman et al.<sup>[40]</sup> The large O—O distance of 1.680 Å has been optimized in the singlet state while the authors<sup>[40]</sup> optimized the 8 type in the triplet state with much shorter O—O distances of 1.3–1.4 Å. Our second model, which is very similar to the zigzag or 5-type model,<sup>[41]</sup> is named by us as “5+” because of a closer position of one of two Cu atoms to the O—O group (Table 6). It leads to the Cu—O distances of 2.020 Å for one Cu atom and of 1.809 or 2.015 Å for another Cu atom in CuMOR. The Cu—O distances are a bit longer

**Table 5.** Relative stabilities (kcal/mol) between singlet and triplet species  $\Delta E_{ST} = E(^3Cu_2O_x) - E(^1Cu_2O_x)$  in various cluster models using B3LYP (or RMP2(FC))/6-31G\* level and CuMOR zeolite at the PBE/PAW level.

X	Cluster	B3LYP	MP2
1	8R	-19.5	38.5
	8RL	-13.8	36.6
	6R+4R	-21.2	18.1
	10T <sup>[a]</sup>	-16.3, -8.3 <sup>[b]</sup> , -7.6 <sup>[c]</sup>	41.0
2	CuMOR <sup>[d]</sup>	-0.4, -1.0 <sup>[e]</sup> , -1.4 <sup>[f]</sup>	-
	8R	-17.9, -11.7 <sup>[f]</sup>	83.0
	6R+4R	-22.3	81.3
	CuMOR <sup>[d]</sup>	-7.8	-

[a] The model is taken from Ref. [15]. [b] M06L.<sup>[43]</sup> [c] B97D.<sup>[20]</sup> [d] PBE<sup>[25]</sup>/PAW using VASP5.3. [e] PBEsol.<sup>[26]</sup> [f] PW91.<sup>[27]</sup>

in the 8R cluster at the B3LYP level as 2.234 Å and 1.963 or 2.324 Å, respectively. This geometry deviation leads to shifted frequencies (500.7 and 1134.5 cm<sup>-1</sup> for Cu—O and O—O vibrations) attributed to this zigzag or 5 complex in Ref. [23] as 561 and 832 cm<sup>-1</sup>, respectively, at the B3LYP level. These 5- and 8-type states were located at electronic surface of triplet <sup>3</sup>B character<sup>[40]</sup> (as confirmed by us at the MP2 level) but which should be less stable than the 6- and 7-type geometries belonging to the electronic surface of singlet <sup>1</sup>A character<sup>[40]</sup> within the Cu...Cu interval studied in our work. The 7-type model is the plain rhombohedra without the internal O—O bond. We have not obtained the 6- and 7-type models in our calculations herein but they are very similar to the alkaline earth MO<sub>2</sub>M species, M = Mg, Ca, Sr, and Ba,<sup>[17,18,44,45]</sup> also having singlet ground state. The reason of the absence of 6- and 7-types can be explained by the different models used herein and in Ref. [40] which lead to different spatial restrictions for the CuO<sub>2</sub>Cu species. One should note that the Cu...Cu interval studied herein with 8R model (Table 6) allows more freedom for typical 6- and 8-models according to the distances of 3.5–3.8 and 3.2–3.4 Å, respectively, assigned to them from the experimental data for the complexes with such groups in the Ref. [23] compared with those of the model by Goodman et al.<sup>[40,41]</sup>

At practice, the obtained MP2 and DFT difference signifies that we operate with the singlet state for the systems using hybrid or GGA DFT methods, but this state is ground one at the MP2 level

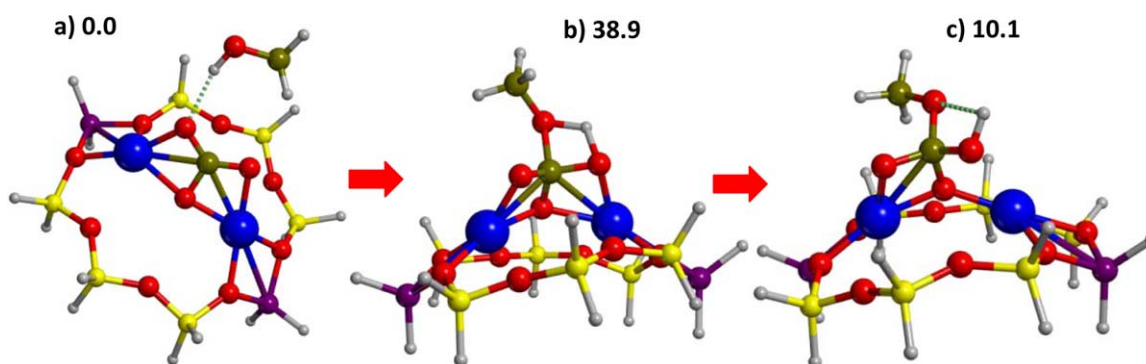


**Figure 3.** Geometries of a) reagent, b) TS, and c) product of the reaction between copper carbonate with methanol optimized at the B3LYP/6-31G\* level. The energies (kcal/mol) are shown relative to the one of the reagent. The atomic color agreement is given in Figure 1.

**Table 6.** The geometries (Å) of the CuO<sub>2</sub>Cu species of different types<sup>[a]</sup> in the various clusters and CuMOR zeolite with *N* atoms of Al per the cluster or per UC at the B3LYP/6-31G\* and PBE/PAW levels.

Cluster	Type <sup>[a]</sup>	CuO <sub>2</sub> Cu		CuOCu	
		Cu...Cu	O—O	Cu...Cu	
8R	5+	3.332	1.314	3.947, 3.285 <sup>[c]</sup>	
	8	3.319 <sup>[b]</sup> , 3.192 <sup>[c]</sup>	1.680 <sup>[b]</sup> , 1.583 <sup>[c]</sup>		
6R+4R	8	3.600, 3.540 <sup>[d]</sup> , 3.309 <sup>[b]</sup>	1.391, 1.431 <sup>[d]</sup> , 1.680 <sup>[b]</sup> ,	3.401, 3.332 <sup>[b]</sup>	
MOR	5+	3.867	1.396	3.291, 3.358 <sup>[c]</sup> , 3.295 <sup>[e]</sup> , 3.349 <sup>[c,e]</sup> , 3.298 <sup>[d]</sup> , 3.360 <sup>[c,d]</sup>	
Exper. <sup>[f]</sup>	6	3.54	1.41	3.29	

[a] According to the classification induced by Goodman et al.<sup>[37]</sup> [b] RMP2/6-31G\*. [c] Triplet state. [d] PW91.<sup>[27]</sup> [e] PBEsol.<sup>[26]</sup> [f] From Ref. [39] for CuO<sub>2</sub>Cu; calculated at the UB3LYP/6-311G\* level<sup>[15]</sup> for CuOCu.

and not at the DFT one. It signifies that we can apply DFT for a calculation of isolated singlet state but we cannot consider reactions in which the multiplicity of the system changes. The relative “singlet-triplet” energies are inverted with DFT methods (Table 5). That is why it is risky to apply DFT for such relevant process as the trapping of O<sub>2</sub> molecules by binuclear copper clusters. This reaction will be accompanied by the change of multiplicity from triplet to singlet in adsorbed state as happens for example at the Si(100) plane.<sup>[46]</sup> The effect of the following reaction depends on the spin state of the involved system. Many aspects of such triplet to singlet transformation require more efforts to be understood even for this simpler system as well as for zeolites.

### The Cu-carbonate formation reaction

As was mentioned in Refs. [12,13], the presence of Cu-formates is a usual sign of the DMC formation from CO and CH<sub>3</sub>OH in CuY zeolite. The IR spectra of Cu-formates are, however, pretty similar to those of the Cu-carbonates. The latter can be tested as the reagents with methanol if they can be easily reproduced under the reaction conditions and if their IR spectra coincide to that earlier observed and assigned to Cu-formates.<sup>[12,13]</sup> The reaction conditions include a formation of water as byproduct. Hence, we should check if the Cu-carbonate formation is not blocked by excessive water. Such analysis is supplied for shortness in Supporting Information (Water influence on Cu-carbonate formation section).

**Table 7.** The Cu—O—Cu<sup>[a]</sup> angles (°) of the CuO<sub>2</sub>Cu (of the 8-type only according to the classification by Goodman et al.<sup>[37]</sup>) and CuOCu species in the various clusters at the B3LYP/6-31G\* level and in CuMOR at the PBE/PAW level.

System	Type	Cu—O <sub>2</sub> —Cu	Cu—O—Cu
8R	B3LYP	— <sup>[b]</sup>	139.48
	MP2	126.79 <sup>[c]</sup>	147.19, 135.09 <sup>[c]</sup>
6R+4R	B3LYP	143.99, 142.23 <sup>[d]</sup>	146.31
	MP2	147.30	136.82
MOR	PBE	123.75	141.91, 147.05 <sup>[c]</sup> , 146.75 <sup>[c]</sup> , 151.79 <sup>[c,e]</sup> , 142.45 <sup>[d]</sup> , 147.53 <sup>[c,d]</sup>

[a] Through the O<sub>cm</sub> center of the O—O bond. [b] Only “5+” geometry was optimized. [c] Triplet state. [d] PW91(6-31G\* for the cluster models). [e] PBEsol.

As we have obtained (see Water influence on Cu-carbonate formation section of Supporting Information), the presence of one water molecule per Cu—O—Cu site increases as much as twice the activation barrier of the CO<sub>2</sub> addition to the Cu—O—Cu. But absolute barrier value (5.18 kcal/mol) remains small at rather higher temperatures of the carbonylation reaction. Hence, the complete dehydration is not required for the reaction cycle.

### Modeling reaction between Cu-carbonates and CH<sub>3</sub>OH

The main interest to the Cu-carbonates in this study is their possible participation in the DMC formation via a two-step reaction with CH<sub>3</sub>OH in Cu-form zeolites. The Cu-carbonate optimized in the 8R cluster at the B3LYP/6-31G\* level seems to possess very close BS values of 220–230 cm<sup>-1</sup> (as evaluated above from the Figure 1 of Ref. [5] in the Cu-carbonate formation reaction section) relative to those observed in IR spectra of CuY<sup>[12,13]</sup> where such species reveal in the course of the carbonylation. Respective reaction of the CuCO<sub>3</sub>Cu(8R) cluster with first CH<sub>3</sub>OH molecule was tested by us (Fig. 3). It corresponds to rather high activation barrier that varies between 46.4 (M06L<sup>[43]</sup>) and 33.7 (LC-wPBE<sup>[47]</sup>) kcal/mol depending on the DFT functional applied (Table 8). The elementary step corresponds to proton transfer with high enough imaginary frequency (Table 8) and is accompanied by carbon C(sp<sup>2</sup>) → C(sp<sup>3</sup>) hybridization shift. The calculated barriers exceed the known experimental value of 14.8 kcal/mol for CuY.<sup>[48]</sup> This result requires additional calculations with PBC and with the cluster approach.

**Table 8.** The energies (kcal/mol) of the reagents (REA, the energy is accepted as zero), TS, and products (PRO) of the attack of the first CH<sub>3</sub>OH molecule toward carbonate calculated using 6-31G\* basis set with DFT methods available with GAUSSIAN09.

	M06L	B97D	B3LYP	LC-wPBE
REA	0.0	0.0	0.0	0.0
TS	46.4	40.7	38.9	33.7
—iω	1555.9	1450.1	1628.9	1638.0
PRO	17.4	16.2	10.1	−3.1

## Conclusions

Activation energy of 16.8 kcal/mol was obtained for the formation of hydrogen carbonate in NaX zeolite from water and carbon dioxide at the DFT/PBE/PAW level with PBC. This moderate barrier is in agreement with easy formation of carbonates in NaX in the presence of water at room temperature. The stabilization of carbonate with cation's displacements allows explaining of earlier experiment of Bertsch and Habgood<sup>[10]</sup> with different character of the equilibrium between  $\text{HCO}_3^-$  and  $\text{CO}_3^{2-}$  forms on different pressures of  $\text{CO}_2$  (or another gas). DFT calculations for considered binuclear  $\text{CuO}_x\text{Cu}$  clusters,  $X = 1 - 2$ , lead to inverted singlet-triplet states relative to that with MP2 that creates a problem to consider at the DFT level relevant reactions with change of the multiplicity of the system. The presence of water changes the activation barrier for formation of copper carbonate from binuclear  $\text{CuOCu}$  clusters from  $\text{CO}_2$  but the barrier remains rather small. Any forms of water dissociated at the carbonate or single  $\text{Cu}^{+2}$  cation are less stable thus resembling the behavior of EA cations. The barrier calculated in the isolated cluster approach (8R) exceeds the known experimental value of 14.80 kcal/mol but depends on the DFT functionals that requires additional tests also involving solution with PBC.

## Acknowledgments

The authors thank Computer Complex SKIF of Moscow State University "Lomonosov" and "Chebyshev" for computational time.<sup>[49]</sup> This research used resources of the "Plateforme Technologique de Calcul Intensif (PTCI)" (<http://www.ptci.unamur.be>) located at the University of Namur, Belgium, which is supported by the F.R.S.-FNRS under the convention No. 2.4520.11. The PTCI is member of the "Consortium des Équipements de Calcul Intensif (CÉCI)" (<http://www.ceci-hpc.be>).

**Keywords:** zeolites · carbonylation · DFT · carbonates · carbon dioxide

How to cite this article: A. A. Rybakov, I. A. Bryukhanov, A. V. Larin, G. M. Zhidomirov. *Int. J. Quantum Chem.* **2015**, DOI: 10.1002/qua.24994

 Additional Supporting Information may be found in the online version of this article.

- [1] H. Awala, J. P. Gilson, R. Retoux, P. Boullay, J. M. Goupil, V. Valtchev, S. Mintova, *Nat. Mater.* **2015**, *14*, 447.
- [2] G. D. Pirngruber, P. Raybaud, Y. Belmabkhout, J. Cejka, A. Zukul, *Phys. Chem. Chem. Phys.* **2010**, *12*, 13534.
- [3] A. Martin-Calvo, J. B. Parra, C. O. Ania, S. Calero, *J. Phys. Chem. C* **2014**, *118*, 25460.
- [4] A. V. Larin, A. Mace, A. A. Rybakov, A. Laaksonen, *Microporous Mesoporous Mater.* **2012**, *162*, 98.
- [5] A. V. Larin, I. A. Bryukhanov, A. A. Rybakov, V. L. Kovalev, D. P. Vercauteren, *Microporous Mesoporous Mater.* **2013**, *173*, 15.
- [6] A. V. Larin, *Microporous Mesoporous Mater.* **2014**, *200*, 35.

- [7] I. A. Bryukhanov, A. A. Rybakov, V. L. Kovalev, A. V. Larin, G. M. Zhidomirov, *Dalton Trans.* **2015**, *44*, 2703.
- [8] I. A. Bryukhanov, A. A. Rybakov, V. L. Kovalev, A. V. Larin, *Microporous Mesoporous Mater.* **2014**, *195*, 276.
- [9] P. A. Jacobs, F. H. van Cauwelaert, E. F. Vansant, *J. Chem. Soc. Faraday Trans. 1* **1973**, *69*, 2130.
- [10] L. Bertsch, H. W. Habgood, *J. Phys. Chem.* **1963**, *67*, 1621.
- [11] J. W. Ward, H. W. Habgood, *J. Phys. Chem.* **1966**, *70*, 1178.
- [12] J. Engeldinger, C. Domke, M. Richter, U. Bentrup, *Appl. Catal. A Gen.* **2010**, *382*, 303.
- [13] J. Engeldinger, M. Richter, U. Bentrup, *Phys. Chem. Chem. Phys.* **2012**, *14*, 2183.
- [14] M. J. Frisch, G. W. Trucks, H. B. Schlegel, G. E. Scuseria, M. A. Robb, J. R. Cheeseman, G. Scalmani, V. Barone, B. Mennucci, G. A. Petersson, H. Nakatsuji, M. Caricato, X. Li, H. P. Hratchian, A. F. Izmaylov, J. Bloino, G. Zheng, J. L. Sonnenberg, M. Hada, M. Ehara, K. Toyota, R. Fukuda, J. Hasegawa, M. Ishida, T. Nakajima, Y. Honda, O. Kitao, H. Nakai, T. Vreven, J. A. Montgomery, Jr., J. E. Peralta, F. Ogliaro, M. Bearpark, J. J. Heyd, E. Brothers, K. N. Kudin, V. N. Staroverov, R. Kobayashi, J. Normand, K. Raghavachari, A. Rendell, J. C. Burant, S. S. Iyengar, J. Tomasi, M. Cossi, N. Rega, J. M. Millam, M. Klene, J. E. Knox, J. B. Cross, V. Bakken, C. Adamo, J. Jaramillo, R. Gomperts, R. E. Stratmann, O. Yazyev, A. J. Austin, R. Cammi, C. Pomelli, J. W. Ochterski, R. L. Martin, K. Morokuma, V. G. Zakrzewski, G. A. Voth, P. Salvador, J. J. Dannenberg, S. Dapprich, A. D. Daniels, Ö. Farkas, J. B. Foresman, J. V. Ortiz, J. Cioslowski, D. J. Fox, Gaussian 09, Revision A.1; Gaussian, Inc.: Wallingford, CT, **2009**.
- [15] J. S. Woertink, P. J. Smeets, M. H. Groothaert, M. A. Vance, B. F. Sels, R. A. Schoonheydt, E. I. Solomon, *Proc. Natl. Acad. Sci. USA* **2009**, *106*, 18908.
- [16] A. V. Larin, A. A. Rybakov, G. M. Zhidomirov, A. Mace, A. Laaksonen, D. P. Vercauteren, *J. Catal.* **2011**, *281*, 212.
- [17] G. M. Zhidomirov, A. A. Shubin, A. V. Larin, S. I. Malykhin, A. A. Rybakov, In *Practical Aspects of Computational Chemistry I. An Overview of the Last Two Decades and Current Trends*, Vol. XV; J. Leszczynski, M. K. Shukla, Eds.; Springer: Dordrecht, **2012**; pp. 579–644.
- [18] G. M. Zhidomirov, A. V. Larin, D. N. Trubnikov, D. P. Vercauteren, *J. Phys. Chem. C* **2009**, *113*, 8258.
- [19] A. V. Larin, G. M. Zhidomirov, D. N. Trubnikov, D. P. Vercauteren, *J. Mol. Catal. A Chem.* **2009**, *305*, 90.
- [20] S. Grimme, *J. Comput. Chem.* **2006**, *27*, 1787.
- [21] P. J. Smeets, M. H. Groothaert, R. A. Schoonheydt, *Catal. Today* **2005**, *110*, 303.
- [22] M. H. Groothaert, P. J. Smeets, B. F. Sels, P. A. Jacobs, R. A. Schoonheydt, *J. Am. Chem. Soc.* **2005**, *127*, 1394.
- [23] P. Vanelderden, R. G. Hadt, P. J. Smeets, E. I. Solomon, R. A. Schoonheydt, B. F. Sels, *J. Catal.* **2011**, *284*, 157.
- [24] Y. Zhang, D. Briggs, E. de Smitt, A. Bell, *J. Catal.* **2007**, *251*, 443.
- [25] J. P. Perdew, K. Burke, M. Ernzerhof, *Phys. Rev. Lett.* **1996**, *77*, 3865.
- [26] J. P. Perdew, A. Ruzsinszky, G. I. Csonka, O. A. Vydrov, G. E. Scuseria, L. A. Constantin, X. Zhou, K. Burke, *Phys. Rev. Lett.* **2008**, *100*, 136406.
- [27] (a) J. P. Perdew, J. A. Chevary, S. H. Vosko, K. A. Jackson, M. R. Pederson, D. J. Singh, C. Fiolhais, *Phys. Rev. B* **1992**, *46*, 6671; (b) J. Perdew, J. Chevary, S. Vosko, K. Jackson, M. Pederson, D. Singh, C. Fiolhais, *Phys. Rev. B* **1993**, *48*, 4978.
- [28] G. Kresse, D. Joubert, *Phys. Rev. B* **1999**, *59*, 1758.
- [29] G. Kresse, J. Hafner, *Phys. Rev. B* **1993**, *47*, 558.
- [30] G. Kresse, J. Furthmüller, *Phys. Rev. B* **1996**, *54*, 11169.
- [31] (a) G. Henkelman, B. P. Uberuaga, H. Jónsson, *J. Chem. Phys.* **2000**, *113*, 9901; (b) D. Sheppard, R. Terrell, G. Henkelman, *J. Chem. Phys.* **2008**, *128*, 134106.
- [32] P. Ugliengo, D. Viterbo, G. Chiari, *Z. Kristallogr. Cryst. Mater.* **1993**, *207*, 9.
- [33] A. García-Sánchez, C. O. Ania, J. B. Parra, D. Dubbeldam, T. J. H. Vlugt, R. Krishna, S. Calero, *J. Phys. Chem. C* **2009**, *113*, 8814.
- [34] M. M. Lozinska, E. Mangano, J. P. S. Mowat, A. M. Shepherd, R. F. Howe, S. P. Thompson, J. E. Parker, S. Brandani, P. A. Wright, *J. Am. Chem. Soc.* **2012**, *134*, 17628.
- [35] A. A. Rybakov, I. A. Bryukhanov, A. V. Larin, In *Thermodynamic and Kinetic Aspects of Carbonate Formation*, Proceedings of 7th Russian Zeolite Conference; Zvenigorod, Moscow Region, Russia, 2015.
- [36] (a) I. J. Drake, Y. Zhang, D. Briggs, B. Lim, T. Chau, A. T. Bell, *J. Phys. Chem. B* **2006**, *110*, 11654; (b) I. J. Drake, Y. Zhang, M. K. Gilles, C. N.

- Teris Liu, P. Nachimuthu, R. C. C. Perera, H. Wakita, A. T. Bell, *J. Phys. Chem. B* **2006**, 11665.
- [37] C. C. Chao, J. H. Lunsford, *J. Phys. Chem.* **1972**, 76, 1546.
- [38] M. Lo Jacono, G. Fierro, R. Dragone, C. N. R. Sacso, D. Chimica, V. Uni, L. Sapienza, P. A. Moro, X. Feng, J. Itri, W. K. Hall, *J. Phys. Chem. B* **1997**, 101, 1979.
- [39] K. Magnus, H. Ton-That, J. E. Carpenter, In Three-Dimensional Structure of the Oxygenated form of the Hemocyanin Subunit II of Limulus Polyphemus at Atomic Resolution; K. D. Karlin, Z. Tyekla, Eds.; Bioinorganic Chemistry of Copper, Chapman and Hall: New York, **1993**; pp. 143–150.
- [40] B. R. Goodman, K. C. Hass, W. F. Schneider, J. B. Adams, *J. Phys. Chem. B* **1999**, 103, 10452.
- [41] B. Goodman, W. Schneider, K. Hass, J. Adams, *Catal. Lett* **1998**, 56, 183.
- [42] F. Bernardi, A. Bottoni, R. Casadio, P. Fariselli, A. Rigo, *Int. J. Quantum Chem.* **1996**, 58, 109.
- [43] Y. Zhao, D. G. Truhlar, *J. Chem. Phys.* **2006**, 125, 194101.
- [44] A. A. Rybakov, A. V. Larin, G. M. Zhidomirov, D. N. Trubnikov, D. P. Vercauteren, *Comput. Theor. Chem.* **2011**, 964, 108.
- [45] A. V. Larin, G. M. Zhidomirov, D. N. Trubnikov, D. P. Vercauteren, *J. Comput. Chem.* **2010**, 31, 421.
- [46] X. L. Fan, Y. F. Zhang, W. M. Lau, Z. F. Liu, *Phys. Rev. Lett.* **2005**, 94, 016101.
- [47] (a) O. A. Vydrov, G. E. Scuseria, *J. Chem. Phys.* **2006**, 125, 234109; (b) O. A. Vydrov, J. Heyd, A. Krukau, G. E. Scuseria, *J. Chem. Phys.* **2006**, 074106; (c) O. A. Vydrov, G. E. Scuseria, J. P. Perdew, *J. Chem. Phys.* **2007**, 154109.
- [48] X. Zheng, A. T. Bell, *J. Phys. Chem. C* **2008**, 112, 5043.
- [49] V. Sadovnichy, A. Tikhonravov, V. Voevodin, V. Opanasenko, "Lomonosov": Supercomputing at Moscow State University; J.S. Vetter, Ed.; Contemporary High Performance Computing: From Petascale toward Exascale, CRC Press: Boca Raton, **2013**, p. 283.

Received: 30 April 2015

Revised: 4 July 2015

Accepted: 30 July 2015

Published online on Wiley Online Library